Automotive Powertrain DC/DC Converter with 25kW/dm³ by using SiC Diodes

B. Eckardt, A. Hofmann, S. Zeltner, M. Maerz

Fraunhofer Institute of Integrated Systems and Device Technology (IISB),
Schottkystrasse 10, 91058 Erlangen - Germany, www.iisb.fraunhofer.de

Abstract

In this paper a 100kW buck-boost DC/DC converter for use in the powertrains of hybrid cars is presented. Since size and weight of the converter are of essential importance for this application, a target size of 4 liter was defined, resulting in a benchmark power density of 25kW/dm³. Currently available silicon carbide Schottky diodes allow switching frequencies of up to 100kHz when combined with ultra-fast 600V IGBTs. This switching frequency, however, is not sufficient to realize the necessary size reduction. A polyphase approach has been chosen therefore. Twelve phases shift the fundamental frequency of the input and output ripple voltage above one megahertz, resulting in a great size reduction of the passive components. The converter operates with a coolant temperature of up to 85°C without derating. An overview of the converter design is given as well as loss and efficiency calculations.

1. Introduction

The development of ultra low emission vehicles (ULEV) is a great challenge for the automotive industry and becomes more and more a technology driver for power electronics.

Key components, whether talking about electric, hybrid or fuel cell cars, are powerful and highly efficient DC/DC converters. Measurements clearly show power savings of up to 24% for inner city driving by the recuperation of braking energy [1].

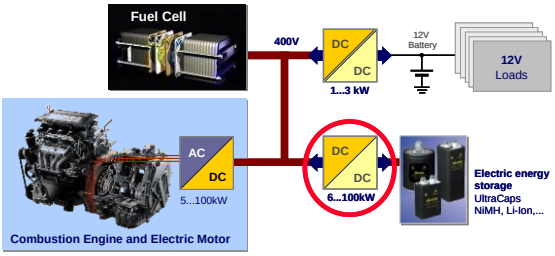

Figure 1: Hybrid powertrain with high power DC/DC converter

Pure electric vehicles suffer from a limited cruising range because of the low energy density of batteries in comparison to conventional fuels. A more attractive approach are hybrids, using fuel – in a combustion engine or a fuel cell – to supply the continuous power demand, and an electrical energy storage system for recuperation.

Batteries are not always the storage of choice for traction applications, because they can not be charged rapidly and survive only a limited number of charge/discharge cycles. In comparison, ultra-capacitors can withstand very high charge and discharge currents and provide a nearly unlimited number of cycles.

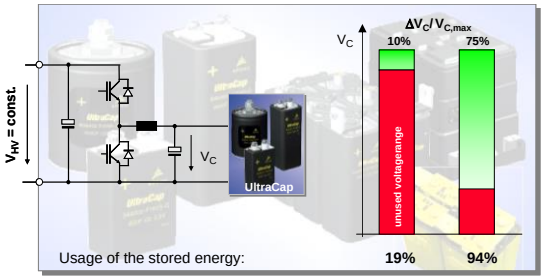

Figure 2: A DC/DC converter realizes an "ideal" electrical energy storage with constant terminal voltage

The main problem with capacitors is that the terminal voltage greatly changes as a function of the stored energy. A direct coupling with the drive requires an inverter with a very high current rating. All our system evaluations have shown that inserting a DC/DC converter between the capacitor and the drive inverter leads to reduced overall system costs.

2. Converter Topology

We have set the aim to realize an ultra-compact converter that, should the situation arise, could be directly integrated into an electrical storage unit.

In order to cover a wide range of applications, we specified a flexible voltage range from 100V to V_1 for the low voltage side (V_{LV}), and from V_1+10V to 450V on the high voltage side (V_{HV}). V_1 is allowed to swing within the whole voltage range during operation. The converter with a nominal output power of 100kW should be capable to handle

currents of up to 300A in both directions, and fit a volume of 4 litres, comparable to the size of a notebook.
A simple non isolating buck-boost converter topology was chosen, because of the low number of passive components. This is especially important because the passive components determine the converter volume. For the given voltage ratio V_{HV} / V_{LV} lower than 4.5:1 the buck-boost topology is the preferred choice.
The main restriction that must be considered in an application is that the voltage V_{LV} must always be lower than the voltage V_{HV} .

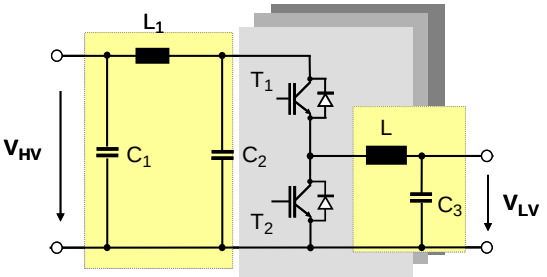

Figure 3: Polyphase buck-boost converter with highside π-filter for EMI suppression

3. Polyphase Concept

Using N phases for a DC/DC converter provides several advantages over a single phase concept:
The fundamental frequency of the voltage and current ripples at the high and the low voltage DC-links is N times the switching frequency. The ripple current load for both DC-link capacitors is reduced by 1/N. The expense for EMI filters is greatly reduced this way.
In addition, also the total volume of the main inductors is reduced by 1/N, because this volume is directly proportional to the total magnetic energy stored in the magnetic cores according to (1).

$$InductorVolume_{total} \cong \left(\frac{I_{Nenn}}{N}\right)^2 \cdot L \cdot N \qquad (1)$$

On the other hand, a high number of phases also causes some drawbacks. More gate driver circuits and more current sensors for phase current balancing are necessary.
In order to evaluate the optimal number of phases with respect to power density, we calculated the total volumes for the main inductor(s), the control and driver logic, the power modules and bus bars as a function of the phase number N. As shown in Figure 4, a fairly shaped minimum occurs between 7 and 16 phases. With more than about 12 phases the volume for gate drivers and interconnections becomes dominant so that the total converter volume rises again.
Taking all these results into account, we chose N=12. This number is even more favorable because it can be divided by 2, 3, 4 and 6, and thus gives us a great flexibility in forming subgroups of phases. An optimization with respect to EMI and part load efficiency is possible this way.

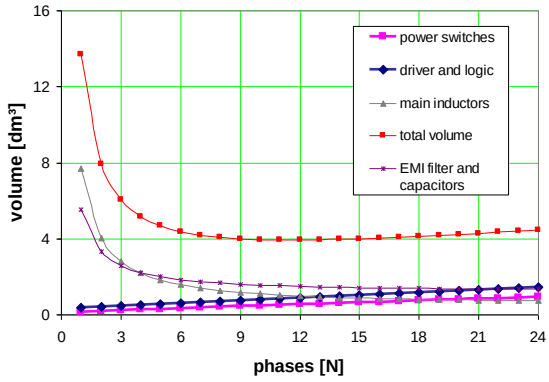

Figure 4: Component volume and total converter volume depending on the number of phases

With N=12, each phase leg must be able to handle a RMS current of 25A in order to meet the output power specifications.
The complex control logic is realized digitally by using a programmable gate array Cyclone II from Altera. This FPGA comprises the pulse pattern generation, 12 current sensor signal filters, and 12 high speed digital current control loops.
The CAN-Bus interface and the voltage control loop are implemented in an Infineon XC164 microcontroller.

4. Switching Frequency

The choice of switching frequency is a trade-off between converter efficiency and volume. MOSFET devices turned out to be unsuitable for the intended application because of the high conduction losses and poor dynamic characteristics of the intrinsic body diodes. We therefore focused on IGBTs in combination with silicon and silicon carbide diodes.
Figure 5 shows the turn-on behavior of a 600V high-speed IGBT-2 from Infineon with both a 600V Si and a SiC diode. With a SiC diode, the turn-on losses are reduced to 1/3 of the losses induced by an ultra-fast 600V Si p/n-diode. The reverse recovery current of the Si diode induces a peak on the IGBT current which leads to high turn-on losses. SiC Schottky diodes have no recovery charge and thus greatly reduce the current peak at hard commutation.

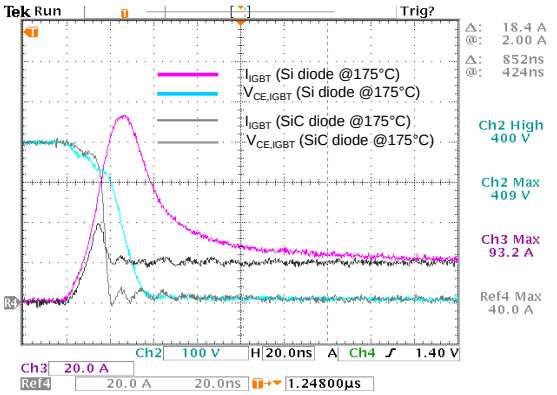

Figure 5: Comparison of the turn-on behavior of a 600V high-speed IGBT with a Si and a SiC diode

In Figure 6 the turn-off behavior is shown. Surprisingly the SiC diode showed minor advantages also in this case, which is presumably resulting from the lack of a forward recovery voltage. This is not relevant with respect to the turn-off losses however, because the dominant part of these losses is caused by the current tail of the IGBT.

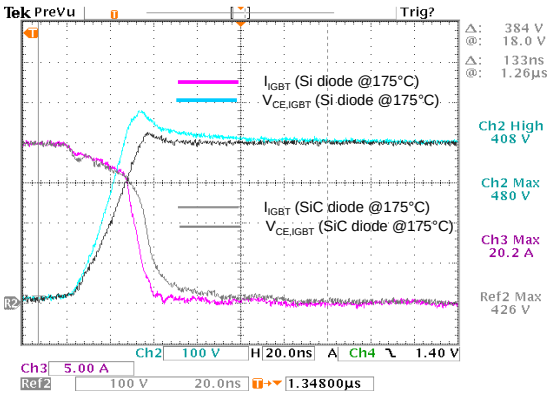

Figure 6: Comparison of turn-off behavior of a 600V high-speed IGBT with a Si and a SiC diode

We evaluated several IGBTs from different semiconductor manufacturers. Missing data from the datasheets were determined by measurings. The switching and conduction losses have been calculated by using MathCAD. The main results are shown in Figure 7 and 8. The currents in these figures correspond to the RMS inductor current.
Due to the superior transient behavior of their diodes, the two devices with SiC diodes show the lowest switching losses. These devices are also the best choice with respect to the total losses. Considering the characteristics in Fig. 8, the advantage in comparison to an all silicon solution is not very large but significant.

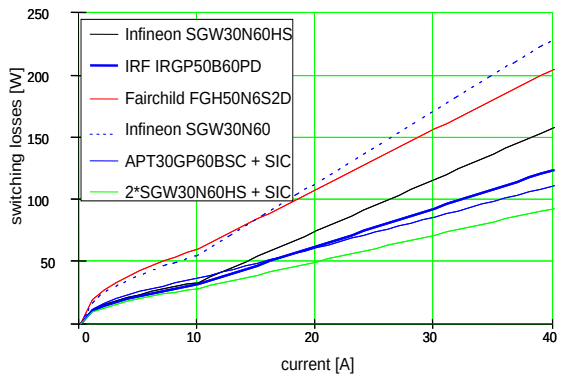

Figure 7: Switching losses of different IGBTs with diode induced losses in the buck mode:
V_{LV}=200V, V_{HV}=400V, R_{Gate}=2Ω, $T_{Junction}$=125°C

In order to achieve the best compromise between power density and efficiency, and for reasons of bare die availability, we decided to use 600V high-speed IGBT-2 and 600V SiC diodes, both from Infineon. The low switching losses of these IGBTs open the way to a switching frequency of 100kHz. Despite the very high saturation voltage of the IGBTs (2.7V), the ratio between switching and conduction losses is still above 3:1.

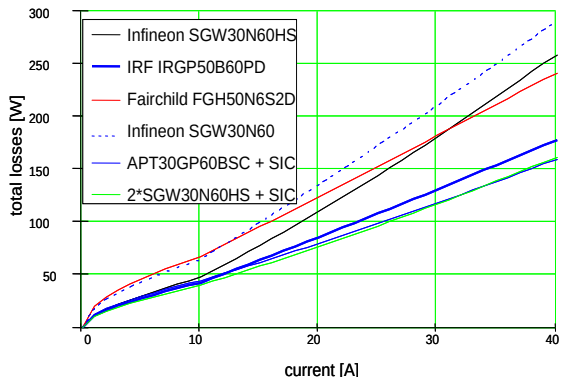

Figure 8: Total power dissipation at 100kHz in buck mode:
V_{LV}=200V, V_{HV}=400V, R_{Gate}=2Ω, $T_{Junction}$=125°C

As can be seen from Figure 8, the total power dissipation in the IGBT switch of one phase leg is about 100W at 400V DC-link voltage and 25A (RMS) inductor current.

5. Efficiency Calculations

With all phases active, the calculated overall efficiency of the converter is higher than 95% for output currents above 40A.
A great advantage of the digital control is the possibility to adopt the number of active phases depending on the actual current demand.
In the example given in Figure 9, the number of active phases is switched from 1 to 3 at 24A, from 3 to 6 at 68A, and from 6 to 12 at 144A. The

increase in efficiency is about 3% at 10% of the maximum output current (30A). At smaller currents the efficiency improvement is even higher, e.g. about 12% at 10A output current.

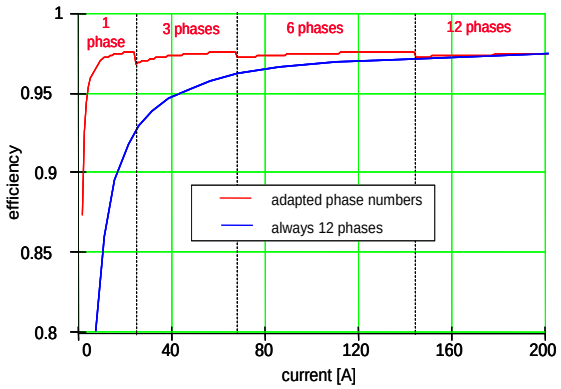

Figure 9: Calculated converter efficiency in buck mode. V_{LV}=280V, V_{HV}=400V

Applying a load depending phase control makes it possible to achieve efficiencies above 97% over a wide load current range (10% to 100%). This is especially important since the converter is operated mainly under part load conditions in the intended automotive applications.

6. Half Bridge Gate Driver

A major drawback of polyphase converters is the expense for gate drivers and current control circuits, that increases proportionally to the number of phases. Very compact half bridge gate driver units had to be developed therefore. On reasons of noise immunity and reliable operation, we decided to use insulating gate driver. Each gate driver had to provide an output power of about 0.5W with peak currents of several amperes. Signal delay and distortion had to fit to a 100kHz PWM.

Figure 10: Thermal image of the new gate driver under full load conditions: 0.5W, 100kHz, 20°C ambient temperature

The fully isolating 600V half bridge gate driver units are mounted on top of the power modules as shown in Figure 12. In order to meet the timing requirements, power and signal transmission were separated in contrast to [3],[4]. Signal transmission is realized with an inductive data coupler IC. The whole secondary side functionality (V_{CE} detection, UVLO, etc.) is integrated in the SKIC1003 from Semikron. An additional bipolar stage (Zetex) boosts the peak current capability. The electrical power for the secondary side is supplied via a single transformer with separate windings.

The thermally stressed gate resistors are located closely to the liquid cooled mounting frame. The resistors reach a ΔT of max. 50°C above coolant temperature at full load, as shown by the thermal image in Figure 10. The size of the driver unit, including an isolating transmission for the current sensor (shunt) signal, is 43mm x 24mm x 12mm, and thus takes no more area than the DCB substrate with the corresponding power semiconductors.

7. Passive Components

Aiming on a power density of 25kW/dm³, it is no longer possible to use standard passive components. For the main inductors, we evaluated several different types of chokes, based on cores of ferrite, amorphous materials and MPP. The target was to minimize the inductor volume under constraints like a high saturation current and low overall losses. Four of the inductors are shown in Figure 11, the technical data of these inductors are summarized in Table 1. We decided to use a toroidal choke with an amorphous material core because of cost, size and availability reasons.

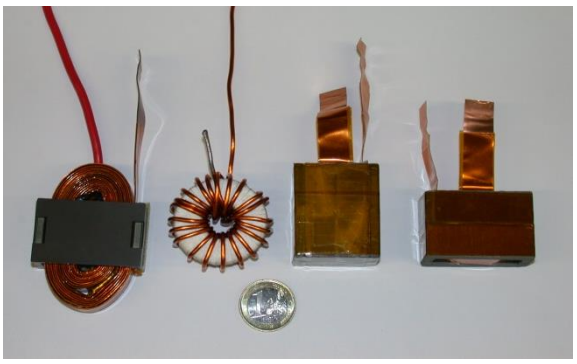

Figure 11: Four samples of the tested main inductors

With the chosen inductor design the copper losses are dominating. In order to provide an efficient cooling of the outward windings, the choke was molded in a metal housing.

The DC-link capacitor C_2 is divided in four separate capacitor banks with 30uF each. Three phases are

connected to each capacitor bank, resulting in a fundamental frequency of the ripple voltage of 300kHz. Each capacitor bank is coupled to the common DC-link capacitor C_1 (300uF) via filter inductors (0.1uH).

Table 1: Overview of four evaluated inductors

Inductor	Ferrite ELP Core	Ring Core	MPP Core 1	MPP Core 2
Material	Ferrite N87	Amorph.	MPP	MPP
Core Type	ELP43	ring	special	special
Dimensions Including windings	43 x 64 x 21mm³	∅43 mm x 23mm	35 x 42 x 23mm³	43 x 30 x 22,5mm³
Volume	57.8cm³	33.4cm³	33,8cm³	29cm³
Windings	16	22	24	24
Serial Resistance at 100kHz	890mΩ	1230mΩ	740mΩ	510mΩ
Saturation current	44A	65A	soft	soft
Inductance	40µH	54µH	48µH @ 35A	46µH @ 35A
costs	low	high	very high	very high

This DC-link design keeps the physical dimensions of the passive components small, prevents internal oscillations, and provides an effective EMI filter characteristic.
All capacitors in both DC-links are stacked foil capacitors. Compared to electrolytic capacitors they have a very high ripple current capability and no durability problems when operated at elevated temperatures.
With the brick shape of the foil capacitors, the available volume can be used very efficiently. Both DC-links comprise a capacitance of 420µF/450V, which could be realized in a volume of about 350cm³ each. This capacitance is necessary to stabilize the control loop and to withstand a load dump under full current and high voltage conditions.

8. Mechatronic Integration

The whole converter is integrated into a shielding aluminium housing according to IP64. The mechanical design was performed using the 3D construction tool ProEngineer.
Micro coolers were chosen because of their very small volume and low thermal resistance. A special transversal flow cooler design has been developed together with Curamik.

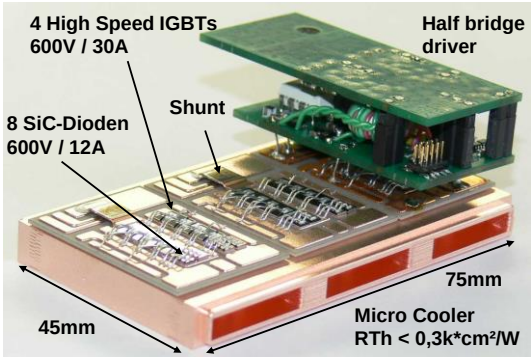

Figure 12: Three DCB substrates, one with half bridge driver, mounted on a micro cooler

The dimensions of the micro cooler are 75mm x 45mm, with a thickness of only 7mm. Three substrates, each comprising an IGBT half-bridge, are mounted on a single cooler. Four of these coolers are used in the converter. The thermal resistance is about 0.3Kcm²/W. By construction, the water inlet of the micro coolers is arranged directly under the pulse capacitors (C_2) which are loaded with very high ripple currents.

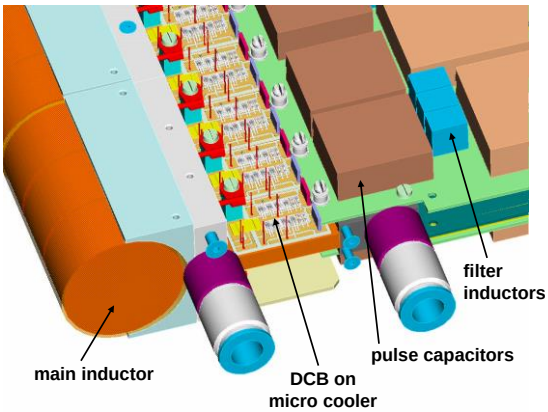

Figure 13: All devices with high power dissipation are thermally coupled to the liquid cooling

The water outlet is designed to cool the twelve main inductors attached directly to the water channel with their aluminium case, as shown in figure 13. The printed circuit boards for the high and the low voltage DC-links are placed sandwich like, with the digital control board in between. With a persisting copper plane on the inside of the PCB sandwich the control board is well shielded against EMI.

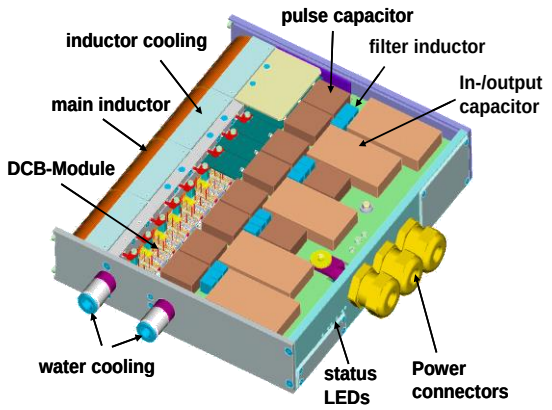

Figure 14: Construction overview on the complete converter

Precise current sensors for the total converter input and output current are integrated in the power terminals. The converter has three power terminals for shielded cables with a copper cross section of 70mm². Two terminals are for the V_{LV} and V_{HV} anode connections and one is for the common negative connection.

9. Comparison of Realized Prototypes

The newly developed converter is 3.5 times smaller than the previous one [1] and provides about 40% more output power.

Table 2: Technical overview on the prototypes

Converter Data	70kW	100kW
Low Side Voltage Range V_{LV}	min.: 200V max.: 290V	min.: 100V max.: V_1
High Side Voltage Range V_{HV}	min.: 300V max.: 450V	min.: V_1+10V max.: 450V
Low Side Current	max.: 280A	max.: 300A
High Side Current	max.: 240A	max.: 270A
Max. Coolant Temperature	85°C	85°C
Switching Freq.	17kHz	100kHz
Phase Number	3	12
Main Inductor	90µH	50µH
Capacitance C_3	6mF	420uF
Capacitance C_1	3mF	300uF
Capacitance C_2	45µF	120µF
Dimensions	360 x 260 x 150 mm³	305 x 260 x 50 mm³
Power Density	5.0W/cm³	25W/cm³
Efficiency 10% to 90% Output Power	92% to 98%	Calculated 97% to 98%

Figure 15: DC/DC converter prototypes
On the left hand side is the new 100KW converter, on the right hand side a state-of-the art 70kW converter

Furthermore the efficiency at low power transfer conditions can be optimised by the adoption of active phases.

10. Conclusion

The designed 100kW DC/DC converter with a power density of 25kW/dm³ is a milestone on the way to compact and highly efficient power electronics for future automotive applications. With the small size and low weight the converter can be easily installed into cars.

The high power density became possible by using latest silicon carbide power semiconductors, new driver units and new passive components, as well as by applying a polyphase concept. The polyphase approach also allows an optimization of the efficiency under light load conditions.

With a sophisticated 3D construction, an efficient cooling of all relevant devices could be achieved as well as an efficient use of the given installation space. The achievements of this development are shown by the comparison to a former converter.

11. Acknowledgment

This work was funded by the Fraunhofer research program „Compact and Efficient Energy Conversion“.

12. References

[1] B. Eckardt, et. al.: “High Power Buck-Boost DC/DC Converter for Automotive Powertrain Applications”, PCIM 2005, Nuremberg, Germany

[2] Gerber M., März M.: “System Integration in Automotive Power Systems”. Proceedings of European Power Electronics Conference (EPE), Dresden, 2005

[3] Patent DE 10 2004 026 052

[4] S.Zeltner, et. al.: “An Isolating IGBT Halfbridge Driver with Embedded Magnetics”, PCIM 2004, Nuremberg, Germany